

# A SECONDARY EMISSION MONITOR IN THE SINQ BEAM LINE FOR IMPROVED TARGET PROTECTION

R. Dölling<sup>†</sup>, M. Rohrer, Paul Scherrer Institut, 5232 Villigen PSI, Switzerland

## Abstract

A 4-strip secondary-emission monitor (SEM) has been installed in the beam line to the SINQ neutron source to detect irregular fractions of the megawatt proton beam which might damage the spallation target. We discuss the estimated performance of the monitor as well as its design and implementation.

## INTRODUCTION

A key issue to ensure safe operation of the SINQ spallation target is to prevent a too large current density of the proton beam at the target. Recently, a campaign has been launched in order to improve the fast detection of such improper beam delivery [1]. Already small beam fractions accidentally bypassing the upstream muon production target TE result in a significant increase of current density at the SINQ target. This 'irregular' beam fraction has not been decelerated and hence is shifted vertically in the dispersive section at wire monitor MHP55X/56Y.

The SEM MHB28 has been placed in the aperture of the wire monitor (Fig. 1) to provide a permanent monitoring of irregular beam in the upcoming beam period. It consists of four parallel foil strips, two above the beam and two below. The basic approach is to fix the position of the main part of the beam by limiting the allowed beam fraction on the inner strips to a few percent. Irregular beam is then prevented by limiting the allowed beam fraction on the outer strips to much less than one percent.

A similar approach, based on the vertical collimator KHNY30 located inside quadrupole QHJ30 1.8 m downstream of MHB28, is already in use [2]. However, its accounted beam fraction is very limited by the heat load and activation tolerated by its uncooled copper blocks. This enforces a wider gap which results in a less strict supervision.

## SETUP

The 20  $\mu\text{m}$  Molybdenum foil strips are pre-tensioned by 1.4310 stainless steel springs with 0.42 and 1.3 N to keep them flat even at strong heating (Fig. 2). The clamps are coated at the outside with Diconite® DL-5 to allow many thermal cycles without sticking in the guide blocks. The guide blocks are isolated with hidden ceramic spacers from the grounded parts of the ring. All parts made from stainless steel. All 8 foil ends are contacted via clamp/spring/guide block and Kapton isolated wire to a 9-pin D-Sub feedthrough at the wire monitor flange. The clamps protrude up to 20 mm into the 200 mm aperture of the adjacent vacuum chamber, which is not critical at the monitor location. Since the electrodes are largely free standing, we don't use an additional biased electrode for pulling the secondary electrons.

The four foil signals are transported via a shielded cable to the LogIV4x4 read-out electronics outside the vault (similar to [3]). The signals from the other foil ends are transported to the electronics rack in the same way. This allows us to check the presence of the foil strips by injecting a test current from a current source (into the normally open ended cable).

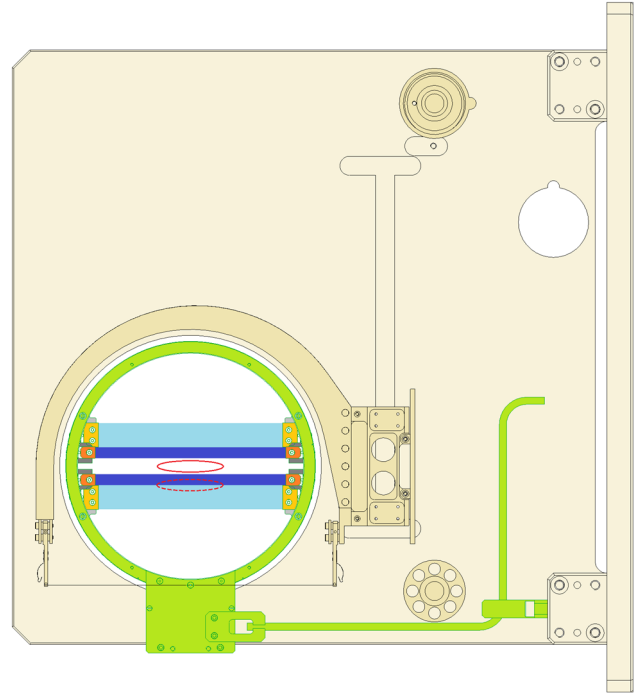


Figure 1: Wire Monitor MHP56Y (front, not all parts shown) and MHP55X (rear side, not visible) with 4-strip SEM MHB28 (green, foil strips blue) inserted and clamped to the base plate.  $2\sigma$  beam contours are indicated for regular (full red) and irregular (dotted red) beam. Beam comes out of drawing plane.

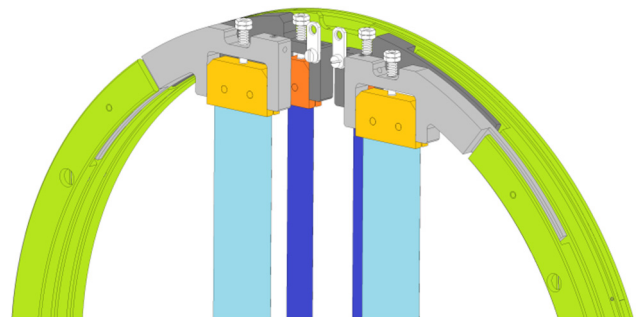


Figure 2: Foil tensioning with springs. Clamps (orange), guide blocks (grey), grounded parts (green), wires not shown. Each spring compressed by 3 mm.

<sup>†</sup> rudolf.doelling@psi.ch

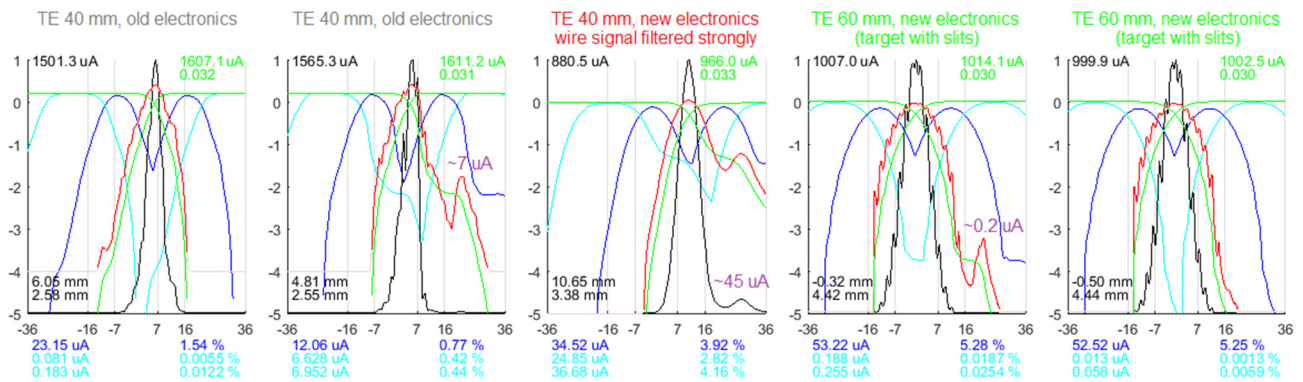


Figure 3: Examples of vertical beam profiles MHP56 with 0/~7/~45/~0.2/0  $\mu\text{A}$  irregular beam current. Horizontal axis: Vertical position in beam pipe [mm]. **Black line**: Wire signal normalized (linear). **Black**: Beam current measured with current monitor MHC6, beam centre position and  $1\sigma$  width. **Red line**: Beam current line density [ $\log(100 \mu\text{A}/\text{mm})$ ]. **Green lines**: Beam current integrated from left and right [ $\log(\text{mA})$ ]. **Green**: Beam current for  $n_{\text{SE}} = 0.030$  and actual secondary emission yield of wire surface  $n_{\text{SE,act}}$ . **Blue line**: Maximum of both beam currents on inner strips when profile position is assumed to be shifted [ $\log(\text{mA})$ ]. **Blue**: close-to-centre minimum of blue line. **Cyan line**: Maximum of both beam currents on outer strips [ $\log(\text{mA})$ ] at same assumed profile shift. **Upper cyan**: Maximum of both beam currents on outer strips at inner-strips-minimum. **Lower cyan**: Same, but in a range of  $\pm 2$  mm around inner-strips-minimum.

### BEAM PROPERTIES, STRIP SIZE AND PERFORMANCE OF SUPERVISION

Beam properties at MHP55X/56Y have been determined from 330 sets of beam profiles taken in the years 2008 - 2017 during beam production and beam development. With the 40 mm thick TE, the  $1\sigma$  beam width is typically  $2.9 \pm 0.9$  mm vertically (and 14-15 mm horizontally). The irregular beam is shifted by 17 mm. Strip sizes and positions are adapted to this situation. They are chosen in a way that the centred regular beam passes both inner strips to a sufficient degree, but practically not the outer strips, while a significant part of the irregular beam passes the lower outer strip. We use a width of 9 mm for the inner strips, of 20 mm for the contiguous outer strips and 14 mm for the central gap.

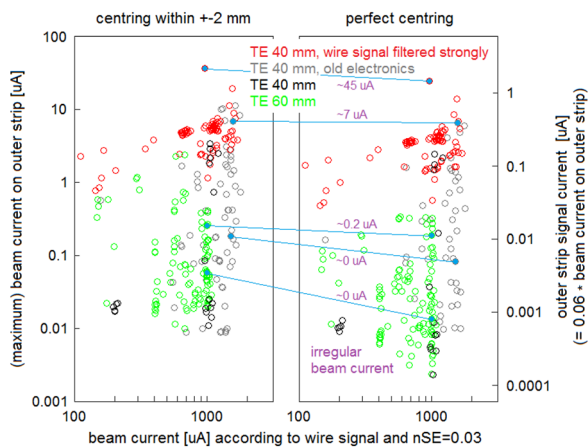


Figure 4: Maximum beam current passing one of the outer strips. The corresponding strip signal currents are estimated on the basis of the average secondary emission yield of  $n_{\text{SE}} = 0.030$  deduced for the surface of the two  $48 \mu\text{m}$  Molybdenum wires of the wire monitor. The five examples from Fig. 3 are marked in blue.

The sensitivity of this setup to irregular beam can be estimated from previously measured profiles using the evaluation depicted in Fig. 3: It is assumed that the beam can be centred vertically (to minimize the maximum of the signal currents of the inner strips) either perfectly or with an accuracy of  $\pm 2$  mm. Under this condition, the beam currents to be expected at the outer strips (the lower cyan numbers in Fig. 3) are given by Fig. 4. Comparison with profile shapes indicate that irregular beam correlates with beam current on the lower outer strip above  $0.1 \mu\text{A}$  for profiles taken with the present wire monitor electronics (black and green points in Fig. 4) and above  $1 \mu\text{A}$  for the former slower and less sensitive electronics (grey points). The irregular beam current is then of the order of the beam current passing the lower outer strip.

Practically, the performance of supervision of irregular beam by the basic approach of just limiting the outer strip signal currents is limited by the quality of vertical beam 'centredness' which can be reached in everyday operation and during beam current ramping. An active beam centring, e.g., on the basis of the position information from the relative difference of the signal currents from the inner strips, could be helpful. To prevent frequent interlocks due to a centring margin of, e.g.,  $\pm 6$  mm, we have to set a correspondingly higher switch off (interlock) limit of  $0.6 \mu\text{A}$ , set in the read-out electronics for the outer strip signal currents, corresponding to an irregular beam fraction of the order of  $10 \mu\text{A}$  (estimated from Fig. 3). Inclusion of position information from the inner strips into the evaluation would improve this. Hereto an algorithm can be derived from a simulation of strip currents assuming a Gaussian vertical beam profile of nominal width.

In the case of sole irregular beam, this supervision will fail, if the associated unusual steering cannot be detected or prevented. At an unexpectedly small vertical width of the regular beam, irregular beam can be limited only by limiting the beam currents to the inner strips. The margin cannot, however, be set as low as needed.

The irregular beam fraction can also be observed in the horizontal beam profile at the next downstream wire monitor as evident in Fig. 5. Due to the overly strong low pass filtering of the signal at that time, the local current density was likely to have been greater increased than it appears.

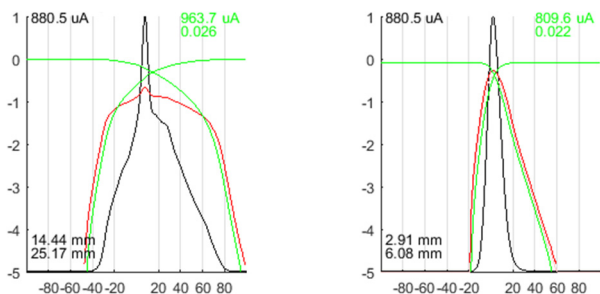


Figure 5: Horizontal (left) and vertical (right) profile at wire monitors MHP57/58, located 6.27 m downstream of MHP55/56, corresponding to the third profile in Fig. 3.

### FOIL PROTECTION

If the 20  $\mu\text{m}$  Molybdenum foil is accidentally hit by the full nominal beam of 1.7 mA, it would not melt even at the lower observed beam width. However, the strips would survive only a few days due to vapour pressure and evaporation at an estimated temperature of  $\sim 1920^\circ\text{C}$  (at assumed emissivity  $\varepsilon = 0.24$ , material data from [4]). Also, foil tension would be lost due to creep within hours. To prevent such damage in the long term, the maximum temperature has to be kept to below  $\sim 1470^\circ\text{C}$  (at  $\varepsilon = 0.19$ ). This can be reached either by reducing the foil thickness to 6  $\mu\text{m}$ , or by reducing the core beam current density. Assuming a Gaussian profile, the latter can be provided by limiting the beam current passing an inner strip to  $\leq 200 \mu\text{A}$ , which is somewhat above the observed values for a centred beam (Fig. 6). However, this requires centring within a margin of  $\pm 4 \text{ mm}$  (estimated from Fig. 3).

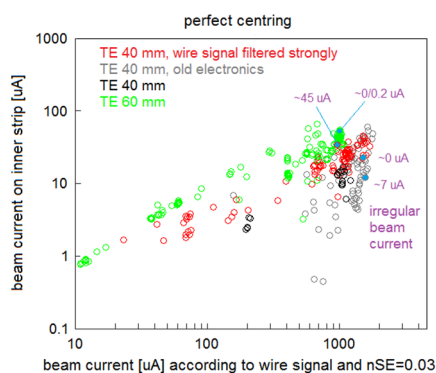


Figure 6: Maximum beam current passing one of the inner strips at centred beam. It is mainly given by current and vertical size of the regular beam.

### SCATTERING AND ACTIVATION

Scattering of the beam by the 20  $\mu\text{m}$  Molybdenum foil strips should be negligible for the further transport according to TURTLE simulations [5].

In the long term, the integrated beam current hitting the strips of MHB28 will be substantial. Activation will be concentrated to the centre part of the strips. At an eventual exchange of the monitors, the strips may be cut away and removed first with a dedicated tool. Since beam losses are comparatively low in this part of the beam line, the surrounding monitor components are much less activated and well accessible [6].

### OUTLOOK

The SEM was installed at the end of the 2018 shut-down (Fig. 7) and will soon be exposed to the production beam. We will learn if vertical position stability and centring will suffice to uphold the mentioned or lower interlock levels, if the downstream beam loss stays unaffected and if radiation damage will occur to the foil. With this we may conclude on the need and feasibility of a harp, covering the full vertical beam profile.

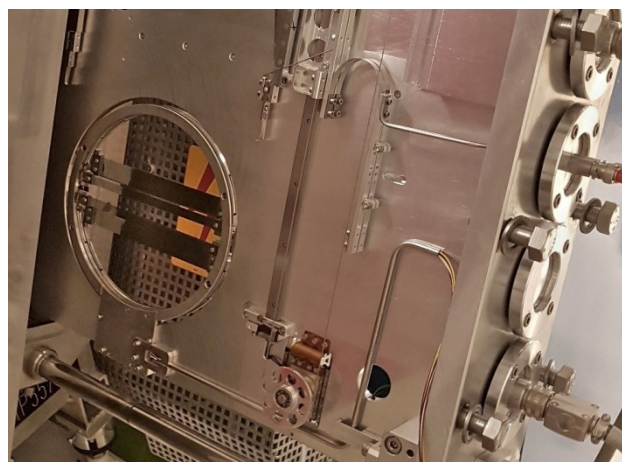


Figure 7: Monitor MHB28 after insertion into MHP55/56.

### ACKNOWLEDGEMENTS

We thank Roger Senn for evaluating the insertion environment, proposing a shift from before to inside the profile monitor, mounting and inserting the monitor, Gregor Gamma for installing the electronics and testing, and Hubert Lutz and Patric Bucher for integration into the machine control system and run permit system.

### AUTHOR CONTRIBUTIONS

RD conceived the device, analysed the data, specified the physics layout and wrote the paper. MR provided the detailed mechanical layout and contributed to the figures.

### REFERENCES

- [1] D. Reggiani *et al.*, “Improving machine and target protection in the SINQ beam line at PSI-HIPA”, in *Proc. IPAC’18*, Vancouver, BC, Canada, Apr.-May 2018, paper WEPAL068.
- [2] U. Rohrer, “First beam tests with the new slit collimator in the proton beam line to SINQ”, PSI, Villigen, Switzerland, Annual Report 2004, Vol. VI, pp. 23-26.
- [3] R. Dölling, “Profile, current and halo monitors of the Proscan beam lines”, in *Proc. BIW’04*, Knoxville, TN, USA, May 2004, *AIP Conf. Proc.*, vol. 732, pp. 244-252, 2004.

Content from this work may be used under the terms of the CC BY 3.0 licence (© 2018). Any distribution of this work must maintain attribution to the author(s), title of the work, publisher, and DOI.

- [4] Plansee Group, Molybdän,  
[www.plansee.com/de/werkstoffe/molybdaen.html](http://www.plansee.com/de/werkstoffe/molybdaen.html)  
[5] D. Reggiani, PSI, private communication, Jan. 2018.

- [6] R. Dölling *et al.*, “Beam diagnostics at the high power proton beam lines and targets at PSI”, in *Proc. DIPAC'05*, Lyon, France, Jun. 2005, paper ITTA02, pp. 228-232.